

**Figure 4** HPLC elution profile of products from the oxidative acylation of 25 mM phenylphosphate using 200 mM thioacetic acid in the presence of 400 mM ferricyanide after 12 h. The reaction was carried out in MES buffer (0.5 M) at pH 7.4. The products were analysed on a C18 reverse-phase HPLC column with a linear gradient of 0–60% acetonitrile (0.1% TFA) at flow rate of 1.0 ml min<sup>-1</sup> for 25 min. The eluate was monitored at 250 nm. Peak I, phenylphosphate; peak II, acetylphenylphosphate. The yield of phenylphosphate was determined by first collecting the material corresponding to each of the peaks in the elution profile and then determining the fraction of the total absorption at 250 nm present in peak II.

recent reports<sup>10,11</sup> The reaction that we describe, although not regioselective, may still find application in peptide synthesis or peptide ligation in aqueous solution but is likely to be of greatest interest in discussions of the origins of life.

If nitriles were formed abundantly in a reducing atmosphere on the primitive Earth as has often been claimed, they could have provided the starting materials for the production of thioacids. The addition of H<sub>2</sub>S to nitriles in organic solvents is a well recognized procedure for the synthesis of thioamides<sup>12</sup>. The reaction would presumably proceed in aqueous solution, although the yields might be lower. Thioamides are hydrolysed in aqueous solution to thioacids in good yield<sup>13,14</sup>. The thioacids are stable in aqueous solution at neutral pHs<sup>15</sup>, and so could have accumulated on the primitive Earth. A simple oxidizing agent could also have formed readily on the primitive Earth, for example Fe<sup>3+</sup> by photooxidation of Fe<sup>2+</sup> (ref. 16). Oxidative acylation eliminates the need for an efficient prebiotic dehydrating agent, thus avoiding many of the problems associated with other proposed methods of acylation.

The assumption that the atmosphere of the Earth was once strongly reducing has been criticized<sup>17</sup>. One alternative source of reduced carbon that has been proposed is reduction of carbon monoxide or carbon dioxide on the surface of transition-metal sulphides<sup>18</sup>. Recent experimental evidence suggests that thioacetic acid is the intermediate in the efficient synthesis of acetic acid (and its activated derivatives) from carbon monoxide on FeS/NiS (ref. 18). It is not clear whether oxidative acylation with thioacetic acid formed in this way is feasible in a prebiotic context, but it is a possibility that should be investigated. □

Received 5 February; accepted 7 July 1997.

- Hulshof, J. & Ponnampereuma, C. Prebiotic condensation reactions in an aqueous medium: a review of condensing agents. *Orig. Life Evol.* **7**, 197–224 (1976).
- Ferris, J. P. in *Cold Spring Harbor Symposia on Quantitative Biology* 29–35 (Cold Spring Harbor Lab. Press, Cold Spring Harbor, NY, 1987).
- Hawker, J. R. J. & Oro, J. Cyanamide mediated syntheses of peptides containing histidine and hydrophobic amino acids. *J. Mol. Evol.* **17**, 285–294 (1981).
- Weber, A. L. & Orgel, L. E. The formation of peptides from glycine thioesters. *J. Mol. Evol.* **13**, 193–202 (1979).
- Weber, A. L. Formation of pyrophosphate, tripolyphosphate, and phosphorylimidazole with the thioester, n,s-diacetyl-cysteamine, as the condensing agent. *J. Mol. Evol.* **18**, 24–29 (1981).
- de Duve, C. *Blueprint for A Cell: The Nature and Origin of Life* (Patterson Publishers, Carolina Biological Supply Co., Burlington, NC, 1991).
- Keller, M., Blöchl, E., Wächtershäuser, G. & Stetter, K. O. Formation of amide bonds without a condensing agent and implications for origin of life. *Nature* **368**, 836–838 (1994).
- Wieland, T. in *The Roots of Modern Biochemistry: Fritz Lipmann's Squiggle and its Consequences* (eds Kleinkauf, H., von Dohren, H. & Lothar, J.) 213–221 (de Gruyter, Berlin, 1988).
- Sheehan, J. C. & Johnson, D. A. The synthesis and reactions of N-acyl thiol amino acids. *J. Am. Chem. Soc.* **74**, 4726–4727 (1952).
- Dawson, P. E., Muir, T. W., Clark-Lewis, I. & Kent, S. B. H. Synthesis of proteins by native chemical ligation. *Science* **266**, 776–779 (1994).
- Liu, C., Rao, C. & Tam, J. P. Acyl disulfide-mediated intramolecular acylation for orthogonal coupling between unprotected peptide segments. Mechanism and application. *Tetrahedron Lett.* **37**, 933–936 (1996).
- Smith, P. A. S. *The Chemistry of Open-chain Organic Nitrogen Compounds* 165–166 (Benjamin, New York, 1965).
- Rosenthal, D. & Taylor, T. I. A study of the mechanism and kinetics of the thioacetamide hydrolysis reaction. *J. Am. Chem. Soc.* **79**, 2684–2690 (1957).
- Butler, E. A., Peters, D. G. & Swift, E. H. Hydrolysis reactions of thioacetamide in aqueous solutions. *Anal. Chem.* **30**, 1379–1383 (1958).
- Cefola, M., Peter, S. S., Gentile, P. S. & Celiano, R. A. V. Rate of hydrolysis of thioacetic acid in basic solution. *Talanta* **9**, 537–542 (1962).
- Braterman, P. S., Cairns-Smith, A. G. & Sloper, R. W. Photo-oxidation of hydrated Fe<sup>2+</sup>—significance for banded iron formations. *Nature* **303**, 163–164 (1983).
- Whittet, D. C. B. Is extraterrestrial organic matter relevant to the origin of life on earth? *Orig. Life Evol. Biosphere* **27**, 249–262 (1997).
- Huber, C. & Wächtershäuser, G. Activated acetic acid by carbon fixation on (Fe, Ni)S under primordial conditions. *Science* **276**, 245–247 (1997).

**Acknowledgements.** We thank A. R. Hill for technical assistance and S. Bailey for manuscript preparation. This work was supported by NASA.

Correspondence and requests for materials should be addressed to L.E.O.

## RNA-catalysed carbon-carbon bond formation

Theodore M. Tarasow, Sandra L. Tarasow & Bruce E. Eaton

NeXstar Pharmaceuticals, Inc., 2860 Wilderness Place, Boulder, Colorado 80301, USA

The ‘RNA world’ hypothesis<sup>1–3</sup>, which assumes that the chemical processes that led to the appearance of life were carried out by RNA molecules, has stimulated interest in catalytic reactions involving oligonucleotides such as catalytic RNA (ribozymes)<sup>4</sup>. Naturally occurring ribozymes have, for example, been shown to efficiently catalyse the formation and cleavage of nucleic-acid phosphodiester bonds<sup>4–8</sup>, and this narrow range of RNA-catalysed reactions has been subsequently expanded by *in vitro* selection methods to include ester<sup>9</sup> and amide<sup>10,24</sup> bond formation S<sub>N</sub>2 reactions and porphyrin metallations<sup>11,12</sup>. Carbon-carbon bond formation and the creation of asymmetric centres are both of great importance biochemically, but have not yet been accomplished by RNA catalysis. A widely used reaction that creates two new carbon-carbon bonds and up to four stereo-centres is the Diels–Alder cycloaddition, which occurs between a 1,3-butadiene and an alkene. Here we report the successful application of *in vitro* selection to isolate pyridine-modified RNA molecules that catalyse a Diels–Alder cycloaddition. We find that the RNA molecules accelerate the reaction rate by a factor of up to 800 relative to the uncatalysed reaction.

The Diels–Alder reaction investigated in this study is shown in Fig. 1, which also shows the modified reactants. The *in vitro* selection (SELEX) for RNA molecules with Diels–Alder activity

(DAase activity) was carried out with a library of  $\sim 10^{14}$  unique sequences. The RNA molecules were constructed of a contiguous 100-nucleotide randomized region, flanked by constant sequence segments to allow for amplification and other enzymatic processes. The RNA was modified by substituting 5-pyridylmethylcarbamid-UTP<sup>13</sup> (compound **2** in Fig. 1) for UTP in the transcription

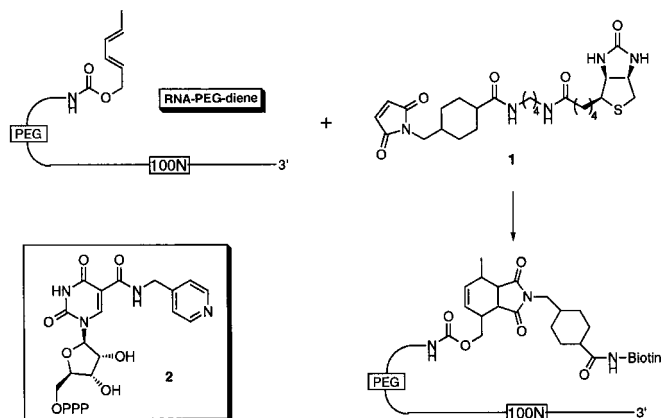


**Figure 1** The Diels-Alder reaction between the acyclic diene conjugated to the RNA through a long PEG linker and the maleimide dienophile **1** (BMCC). The RNA library was prepared with a 100-nucleotide random region (100N). Biotin represents the portion of BMCC not shown in the cycloadduct. Also shown is the structure of the pyridyl methyl *n* modified UTP (**2**) substituted for native UTP during transcription; OPPP represents the triphosphate moiety.

reaction. Pyridyl-modified uridine **2** was chosen to augment the hydrogen-bonding groups of native RNA, to furnish additional hydrophobic and dipolar interactions, and to provide metal coordination sites unlike any contained in unmodified RNA. Previous attempts at isolating RNA DAases were unsuccessful using unmodified oligonucleotide libraries<sup>14</sup>. To allow for selection based on the ability to perform the desired chemistry, RNAs were coupled to an acyclic diene through a long polyethylene glycol (PEG; MW average relative molecular mass ( $M_r$ ) 2,000) linker. The flexible PEG linker was used to provide the diene with the opportunity to access the RNA surface and mimic a diene substrate free in solution.

Rounds of *in vitro* selection for DAase activity were conducted by incubating the RNA-diene construct with the maleimide dienophile (compound **1** in Fig. 1; BMCC) in the presence of transition metals that could form pyridyl-Lewis acid complexes and/or coordinate to the RNA to enhance tertiary structure. The maleimide was attached to biotin so that RNA DAases could be partitioned away from unreacted RNA using streptavidin binding and denaturing polyacrylamide electrophoresis.

Following 12 rounds of *in vitro* selection, the amount of Diels-Alder reaction observed in the presence of the RNA increased from 2.4% in 8 h to 3.3% in 3 min. Subsequently, the library was cloned and bidirectionally sequenced. From the 46 sequences obtained, eight non-clonally derived families were identified. One family comprised 59% of the library population while the other seven unique sequences ranged in representation from one to six of the 46 isolates. The random region sequences for representative isolates are shown in Fig. 2a. Computer-assisted local sequence alignment of representatives from each clonal family identified one consensus sequence, UUCUAACGCG, in five of the eight non-clonally derived

**a**

Family 1 (27 members, 59%)

DA-1 GUGAGUGUCUUGUAGAGCGGCGUGAAGAGCUUACGACUCUUCGUGCCGUUUCUAACGCGUGUCCAUGAACCCGUCCUAGUGGGGGGGCGCCUG  
 DA-14 CUGAGUGUCUUGUAGAGCGGUGUGAAGAGCUUACGACUCUUCGUGCCGUUUCUAACGCGUGCCCAUGAACCCUCCUAGUUGGGGGGGCGCCUG  
 DA-22 UUGAGUGUCUUGUAGAGCGGCGUGAAGAGCUUACGACUCUUCGUGCCGUUUCUAACGCGUGCCCAUGAACCCUCCUAGUGGGGGGGCGCCUG  
 DA-47 UUGAGUGUCUUGUAGAGGCGUGAAGAGCUUACGACUCUUCGUGCCGUUUCUAACGCGUGCCCAUGAACCCUCCUAGUGGGGGGGCGCCUG

Family 2 (6 members, 13%)

DA-2 GGCUUCCAGUAUGGAUACCCUUGGGGCUUCUUGUAGACAGCGUAGUUGUUCUAACGCGUAGGCCUGGUGAGGUACGUGUAGAUGCGGUUAUCGAGGG

Family 3 (4 members, 9%)

DA-37 AGGUAGAAUGGGUCCUGAGUGUUAUAACCAAGGUGUCGGGUGACCGGUACGUCUGGUCCUUGGCGUGGCAUUGUGGGGUGUGUCGACUCGGAUUCGG

Family 4 (4 members, 9%)

DA-17 GGGUUGCGGACUUGUAGAAGCGUAGCUUUCUAACGCGGCGGUGUACCGUUGGAGCUCUCGUAUUGGGCCUUCUUGCCUAUAGGUGAAGGGC

Family 5 (2 members, 4%)

DA-24 ACGCGCAUUAAGUGGUCGCCGUCGUCUCGUAACGACGAUAUCGUGUGUUCUUGGCUUUGAGUCUCGUGCAUUGGACUAUGGGACGUCGGGUCUGGGGA  
 DA-7 CGCAUCGGGCGGUGGACGUGUCUUGUGGAUUGUUCUGGGAUUGGCGGAAUGGCGGGCAUUCUAACGCGCGCACCUUGUUGGGGAGCAUUGGUGGGAUGAG  
 DA-10 UCCACACAAAACGGUGGCGAUAGACCUUGUAGACAAUUGCGGCGAAAAGAGAGUCGGUUGUUGUUCUAACGCGAGGCGGGGUGUCUUAUUGGGCC  
 DA-15 GGUGUCGGUACGGUAUCGUCUGGCCAGGAGUCCUUCUGUGUACGGAAGUCGAUUGCUAGCUCGCGCGCGGAAAUGCGGAUUCGGUGGGCA

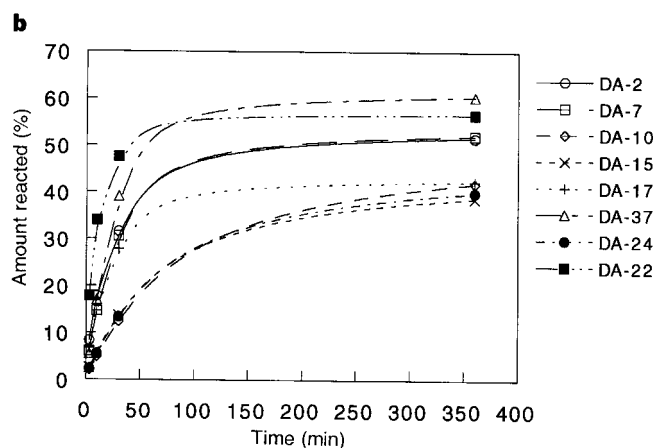


**Figure 2 a**, Random region ( $\sim 100N$ ) sequences of 11 isolates obtained from the DAase *in vitro* selection. Isolates are identified by the number to the left of the sequences. Members of clonal families are labelled (in parentheses) with the total number of family members and the family population as a percentage of the total number of sequences. The computer-identified consensus sequence is in bold and underlined for each of the isolates from families 1, 2 and 4 and the two orphans. **b**, Percentage of individual RNA isolates reacted as a function of time. Isolates are represented by the symbols listed to the right and were incubated with 500  $\mu$ M BMCC for the times indicated.

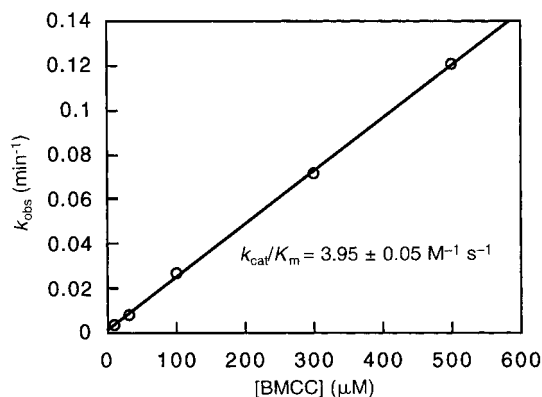


**Figure 3** The observed rate constant ( $k_{\text{obs}}$ ) increases as a function of BMCC concentration for isolate 22. A linear fit of the data yields the line shown ( $y = 0.001545 + 0.0002373x$ ;  $R = 0.9998$ ) with the ratio  $k_{\text{cat}}/K_{\text{m}}$  determined from the slope.

sequences analysed (Fig. 2a). Beyond this limited amount of homology, there are no obvious sequence or structural similarities between the eight non-clonally derived families.

Eight of the isolates shown in Fig. 2a were analysed for their DAase activity. Isolates were kinetically evaluated under solution-saturating concentrations of BMCC (500  $\mu\text{M}$ ). All other conditions were identical to those used during the selection. The results are summarized in Fig. 2b and indicate that each of the isolates tested was capable of facilitating the Diels–Alder reaction, establishing that there were at least eight unique sequences present in the original library that could promote this cycloaddition reaction.

Isolate 22 (DA-22) was chosen for more detailed characterization. Control experiments demonstrated that reaction product formation required both substrates (diene and dienophile). DAase activity was completely dependent on the presence of the pyridyl-modified uridine, as RNA transcribed using the native nucleotide triphosphate was inactive. This is not surprising as the unmodified RNA may have folded into considerably different three-dimensional structures. In addition, the absence of the pyridine groups could have eliminated unique metal-binding sites that effect Lewis acids catalysis.

The insolubility of the dienophile substrate, BMCC, prevented complete Michaelis–Menten kinetic analysis of isolate 22. Nevertheless, kinetic analysis was performed on isolate 22 up to a maximum concentration of 500  $\mu\text{M}$  BMCC (Fig. 3). The data are linear over the range of dienophile concentrations used with a slope equal to  $k_{\text{cat}}/K_{\text{m}}$  ( $3.95 \pm 0.05 \text{ M}^{-1} \text{ s}^{-1}$ ), where  $k_{\text{cat}}$  is the catalytic rate constant and  $K_{\text{m}}$  is the apparent dissociation constant of the RNA–substrate complex. Comparing the apparent second-order rate constant to the uncatalysed rate constant  $k_{\text{uncat}}$  of  $5.42 \times 10^{-3} \text{ M}^{-1} \text{ s}^{-1}$  indicates that isolate 22 achieved an 800-fold rate acceleration of the Diels–Alder cycloaddition. The uncatalysed rate was measured using an identical construct comprised of random pyridine-modified RNA.

Lineweaver–Burke analysis of the data from 30 to 500  $\mu\text{M}$  BMCC gave estimates of  $k_{\text{cat}}$  ( $0.011 \pm 0.002 \text{ s}^{-1}$ ) and  $K_{\text{m}}$  ( $2.3 \pm 0.5 \text{ mM}$ ). Comparison of  $k_{\text{cat}}$  to the second-order rate constant for the uncatalysed reaction,  $k_{\text{uncat}}$ , indicates that isolate 22 has an effective

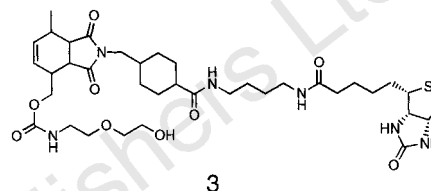
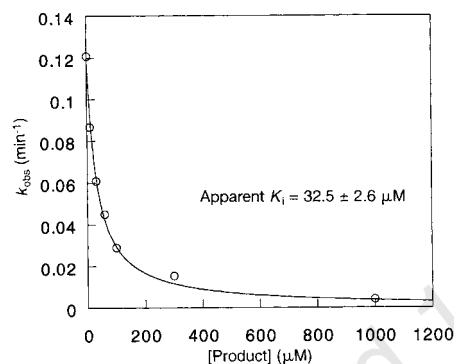


**Figure 4** Inhibition of the DAase activity of isolate 22 by the free cycloaddition product **3** with an apparent  $K_{\text{i}}$  shown. Observed rate constants were measured at increasing concentrations of **3** in the presence of 500  $\mu\text{M}$  BMCC (**1**) and fitted to the equation described in Methods.

molarity of the order of 2 M (ref. 15). Despite a  $K_{\text{m}}$  10-fold higher than the concentration of BMCC (100  $\mu\text{M}$ ) used in the *in vitro* selection, the sequences from Family 1 (see Fig. 2a) seem to have been selected for their ability to increase the reaction rate of bound reactants ( $k_{\text{cat}}$ ) and in effect compensated for a high  $K_{\text{m}}$ . These results clearly indicate that saturating concentrations of substrate are not necessary for the successful selection of RNA catalysts.

Predictably, the free product of the Diels–Alder reaction acts as a reasonably good inhibitor for the RNA-catalysed reaction (Fig. 4). Again, the insolubility of BMCC precluded determination of an absolute inhibition constant ( $K_{\text{i}}$ ), for the product but data collected at 500  $\mu\text{M}$  BMCC and varying amounts of the product (compound **3** in Fig. 4) were used to determine an apparent  $K_{\text{i}}$  of 32.5  $\mu\text{M}$  (ref. 16). Inhibition by the product is consistent with the RNA mediated Diels–Alder reaction occurring in a binding pocket which resembles the product or at least can readily undergo conformational changes to bind the product of the catalysed reaction.

The metal dependence of isolate 22 indicates an absolute dependence on  $\text{Cu}^{2+}$ . No DAase activity was observed in the absence of  $\text{Cu}^{2+}$  even in the presence of the other divalent metals used in the *in vitro* selection. Magnesium, calcium and copper restored DAase activity to  $\sim 71\%$  of that achieved by the complete metal mixture. The additional 29% incremental improvement appears to be a nonspecific metal–RNA interaction that can be accomplished using any of the divalent metals found in the reaction buffer. Titration experiments indicated maximum activity at 10–20  $\mu\text{M}$   $\text{Cu}^{2+}$ , a level similar to that used in the *in vitro* selection (10  $\mu\text{M}$ ). The absolute and specific metal dependence on copper for DAase activity suggests that copper Lewis acid sites are formed as other metal ions present in the reaction buffer could have adopted similar coordination geometries<sup>17,18</sup> resulting in similar RNA structures. The selection of copper in this capacity is consistent with known Lewis-acid-catalysed Diels–Alder reactions in water<sup>19,20</sup>. Indeed, although divalent metal ions have been shown to play an important role in the activity of other oligonucleotide catalysts, such exclusive dependence on  $\text{Cu}^{2+}$  has not been observed.

We used mass spectrometry to identify the DAase reaction product, in order to firmly establish RNA DAase activity<sup>21–23</sup>.

Following reaction of isolate 22 with BMCC, the RNA was isolated by gel filtration and digested with ribonuclease I. The sample was then purified by high-performance liquid chromatography (HPLC) and subjected to electrospray-ionization tandem quadrupole mass spectrometry. From the resulting data, the ion corresponding to the Diels–Alder product was identified (measured  $M_p$ , 630.6; calculated  $M_p$ , 630.8). Moreover, many additional fragment ions were observed which further substantiate formation of the Diels–Alder product. No ions were observed for BMCC reacting with any functional groups on the oligonucleotide, consistent with only the formation of the Diels–Alder cycloadduct.

The methodology used to create these RNA DAases provides a straightforward approach to generating novel catalysts on demand that do not require templating of either substrate. The scope of RNA-catalysed reactions now includes carbon–carbon bond-forming reactions. Although no examples of RNA-catalysed carbon–carbon bond formation were previously known, there appear to be many solutions to [4 + 2] cycloaddition catalysis, as eight unique sequences were found that enhance the rate of the Diels–Alder reaction. These results suggest that similar strategies could be used to identify RNA molecules that catalyse other Diels–Alder reactions, including those with typically unreactive substrates, inverse electron demand Diels–Alder cycloadditions, and hetero Diels–Alder reactions. RNA catalysis of other types of cycloaddition reactions such as dipolar cycloadditions, particularly those benefiting from Lewis acid catalysis, are also possibilities. The ability to expand greatly the functional diversity of RNA through modified bases, to augment accessible chemistries through the use of transition metals, and, perhaps in the future, to include co-factor-assisted transformations, has significant implications for the range of reactions amenable to RNA catalysis. □

#### Methods

**Incubation conditions.** The RNA–PEG–diene construct was prepared by ligating on a PEG–diene modified DNA 10-mer to the 5' end of the RNA using T4 DNA ligase. All RNA incubations were conducted under the following conditions except as noted: 50 mM HEPES, pH 7.0, 500 nM pyridyl methyl-modified RNA, 200 mM NaCl, 200 mM KCl, 1 mM CaCl<sub>2</sub>, 1 mM MgCl<sub>2</sub>, 10 μM each aluminium lactate, Ga<sub>2</sub>(SO<sub>4</sub>)<sub>2</sub>, MnCl<sub>2</sub>, FeCl<sub>2</sub>, CoCl<sub>2</sub>, NiCl<sub>2</sub>, CuCl<sub>2</sub> and ZnCl<sub>2</sub>, 10% ethanol and 2% dimethyl sulphoxide. The concentration of dienophile 1 (BMCC) varied in the isolate characterization experiments, but was held constant at 100 μM throughout the SELEX. Incubations were terminated by the addition of β-mercaptoethanol to a final concentration of 5 mM and/or passing the solution over two successive Nap columns (Pharmacia) to remove excess BMCC.

**Reaction assay and partitioning.** The extent of reaction and partitioning of reacted and unreacted RNA molecules was accomplished using a streptavidin (SA) dependent gel shift. The shifted and unshifted bands were visualized by autoradiography and phosphor-imaging, the latter being used for quantification. For partitioning, shifted bands were excised, the RNA–SA complex extracted, desalted and subjected to reverse transcription and PCR amplification according to standard procedures.

**Kinetic analyses.** All data were obtained at 500 nM RNA and the indicated amounts of BMCC.  $k_{obs}$  values were determined by fitting the fraction of unreacted RNA to the equation for first-order kinetics. The uncatalysed second-order rate of Diels–Alder reaction was measured using random pyridine-modified RNA ( $k_{uncat} = 5.42 \times 10^{-3} \text{ M}^{-1} \text{ s}^{-1}$ ).

**Product inhibition.** Apparent  $K_i$  values for the free cycloaddition product 3 were determined at 500 μM BMCC by fitting the observed first-order rate constants to the following equation for inhibition:  $k_{obs} = (k_{obs0}/2)(\alpha E - I - K_i + ((K_i + \alpha E - I)^2 + 4K_i)^{1/2})$  where  $k_{obs}$  is the measured rate constant in the presence of 3,  $k_{obs0}$  is the observed rate constant in the absence of 3,  $\alpha E$  represents the fractional ( $\alpha$ ) concentration of functional active sites (E),  $I$  is the concentration of 3, and  $K_i$  is the apparent inhibition constant.

Received 23 April; accepted 22 July 1997.

- Joyce, G. F. Ribozymes: Building the RNA world. *Curr. Biol.* **6**, 965–967 (1996).
- Joyce, G. F. The rise and fall of the RNA world. *New Biologist* **3**, 399–407 (1991).

- Joyce, G. F. Some biochemical thoughts on the RNA world. *Chem. Biol.* **3**, 405–407 (1996).
- Cech, T. R. The chemistry of self-splicing RNA and RNA enzymes. *Science* **236**, 1532–1539 (1987).
- Long, D. M. & Uhlenbeck, O. C. Self-cleaving catalytic RNA. *FASEB J.* **7**, 25–30 (1993).
- Bartel, D. P. & Szostak, J. W. Isolation of new ribozymes from a large pool of random sequences. *Science* **261**, 1411–1418 (1993).
- Beaudry, A. A. & Joyce, G. F. Directed evolution of an RNA enzyme. *Science* **257**, 635–641 (1992).
- Kumar, P. K. R. & Ellington, A. D. Artificial evolution and natural ribozymes. *FASEB J.* **9**, 1183–1195 (1995).
- Illangasekare, M., Sanchez, G., Nickles, T. & Yarus, M. Aminoacyl-RNA synthesis catalyzed by an RNA. *Science* **267**, 643–647 (1995).
- Lohse, P. A. & Szostak, J. W. Ribozyme-catalyzed amino-acid transfer reactions. *Nature* **381**, 442–444 (1996).
- Li, Y. & Sen, D. A catalytic DNA for porphyrin metallation. *Nature Struct. Biol.* **3**, 743–747 (1996).
- Conn, M. M., Prudent, J. R. & Schultz, P. G. Porphyrin metallation catalyzed by a small RNA molecule. *J. Am. Chem. Soc.* **118**, 7012–7013 (1996).
- Dewey, T. M., Zyzanski, C. & Eaton, B. E. The RNA world: functional diversity in a nucleoside by carboxyamidation of uridine. *Nucleosides & Nucleotides* **15**, 1611–1617 (1996).
- Morris, K. N. et al. Enrichment for RNA molecules that bind a Diels–Alder transition state analog. *Proc. Natl Acad. Sci. USA* **91**, 13028–13032 (1994).
- Jencks, W. P. in *Catalysis in Chemistry and Enzymology* 644–712 (Dover Publications, New York, 1987).
- Williams, J. W. & Morrison, J. F. The kinetics of reversible tight-binding inhibition. *Methods Enzymol.* **63**, 437–467 (1979).
- Kazakov, S. A. in *Bioorganic Chemistry: Nucleic Acids* (ed. Hecht, S. M.) 244 (Oxford Univ. Press, New York, 1996).
- Cotton, F. A. & Wilkinson, G. *Advanced Inorganic Chemistry* (Wiley, New York, 1988).
- Otto, S., Bertoncin, F. & Engberts, J. B. F. N. Lewis acid catalysis of a Diels–Alder reaction in water. *J. Am. Chem. Soc.* **118**, 7702–7707 (1996).
- Otto, S. & Engberts, J. B. F. N. Lewis acid catalysis of a Diels–Alder reaction in water. *Tetrahedr. Lett.* **36**, 2645–2648 (1995).
- Ni, J., Pomerantz, S. C., Rozenski, J., Zhang, Y. & McCloskey, J. M. Interpretation of oligonucleotide mass spectra for determination of sequence using electrospray ionization and tandem mass spectrometry. *Anal. Chem.* **68**, 1989–1999 (1996).
- Pomerantz, S. C., McCloskey, J. A., Tarasow, T. M. & Eaton, B. E. Deconvolution of combinatorial oligonucleotide libraries by electrospray ionization tandem mass spectrometry. *J. Am. Chem. Soc.* **119**, 3861–3867 (1997).
- Tarasow, T., Tinnermeier, D. & Zyzanski, C. Characterization of oligodeoxyribonucleotide-polyethylene glycol conjugates by electrospray mass spectrometry. *Bioconjugate Chem.* **8**, 89–93 (1997).
- Wiegand, T. W., Janssen, R. C. & Eaton, B. E. Selection of RNA amide synthases. *Chem. Biol.* (in the press).

**Acknowledgements.** We thank L. Gold for support, guidance and vision; the scientific community at NeXstar, especially members of the Medicinal Chemistry group, for helpful discussions and ideas; S. Wayland for the synthesis of compound 2; and T. Wiegand and D. Nieuwlandt for inspiring dialogue and technical assistance. We also thank S. C. Pomerantz, P. F. Crain and J. A. McCloskey for ESI–MS/MS analysis.

Correspondence and requests for materials should be addressed to B.E.E. (e-mail: beaton@nexstar.com).

## Abrupt mid-twentieth-century decline in Antarctic sea-ice extent from whaling records

William K. de la Mare

Australian Antarctic Division, Department of the Environment, Sport and Territories, Channel Highway, Kingston, Tasmania 7050, Australia

A decline in Antarctic sea-ice extent is a commonly predicted effect of a warming climate. Direct global estimates of the Antarctic sea-ice cover from satellite observations, only possible since the 1970s<sup>1–4</sup>, have shown no clear trends. Comparisons<sup>1</sup> between satellite observations and ice-edge charts obtained from early ship records<sup>5</sup> suggest that sea-ice extent in the 1970s was less than during the 1930s, an indication supported by limited regional observations<sup>6</sup>. But these observations have been regarded as inconclusive, owing to the limited spatial and temporal scope of the early records<sup>2</sup>. A significant data source has, however, been overlooked. The southern limit of whaling was constrained by sea ice, and since 1931 whaling records have been collected for every whale caught<sup>7</sup>, giving a circumpolar coverage from spring to autumn until 1987. Here, an analysis of these catch records indicates that, averaged over October to April, the Antarctic summer sea-ice edge has moved southwards by 2.8° of latitude between the mid 1950s and early 1970s. This suggests a decline in the area covered by sea ice of some 25%. This abrupt change poses a challenge to model simulations of recent climate change, and could imply changes in Antarctic deep-water formation and in biological productivity, both important processes affecting atmospheric CO<sub>2</sub> concentrations.